A dendrodendritic reciprocal synapse provides a recurrent excitatory connection in the olfactory bulb

Anne Didier*†, Alan Carleton†‡, Jan G. Bjaalie§, Jean-Didier Vincent‡, Ole Petter Ottersen§, Jon Storm-Mathisen§, and Pierre-Marie Lledo‡¶

*Centre National de la Recherche Scientifique, UMR-5020, Université Claude Bernard, 69622, Villeurbanne Cedex, France; ‡Centre National de la Recherche Scientifique, UPR-2197, 91198 Gif-sur-Yvette Cedex, France; and §Department of Anatomy, Institute for Basic Medical Sciences, University of Oslo, Blindern 0317 Oslo, Norway

Communicated by D. Carleton Gajdusek, Centre National de la Recherche Scientifique, Gif-sur-Yvette, France, March 14, 2001 (received for review January 24, 2001)

Neuronal synchronization in the olfactory bulb has been proposed to arise from a diffuse action of glutamate released from mitral cells (MC, olfactory bulb relay neurons). According to this hypothesis, glutamate spills over from dendrodendritic synapses formed between MC and granule cells (GC, olfactory bulb interneurons) to activate neighboring MC. The excitation of MC is balanced by a strong inhibition from GC. Here we show that MC excitation is caused by glutamate released from bulbar interneurons located in the GC layer. These reciprocal synapses depend on an unusual, 2-amino-5-phosphonovaleric acid-resistant, *N*-methyl-D-aspartate receptor. This type of feedback excitation onto relay neurons may strengthen the original sensory input signal and further extend the function of the dendritic microcircuit within the main olfactory bulb.

The first relay in olfactory information processing is the main olfactory bulb where synaptic transmission between dendrites represents the major mechanism for neuronal interaction (1–5). At this level, synaptic transmission includes both inhibitory and excitatory signals that coexist in a purposeful balance. Inhibition is provided by a reciprocal dendrodendritic circuit that forms the basis for a reliable, spatially localized, recurrent inhibition of mitral cells (MC). Hence, glutamate released by lateral dendrites of bulbar relay neurons, MC, and tufted cells excites the dendrites of local interneurons called granule cells (GC) (6–8), which in turn, release γ-aminobutyric acid (GABA) directly back onto MC (7–10). The extensive lateral dendrites of MC and the possible spread of excitation through GC dendrites provide a mechanism for lateral inhibition (7, 8, 11–13). Finally, because a single GC is believed to contact a large number of MC (14), this reciprocal inhibitory synaptic connection contributes to the synchronization of MC (15–17). As a result, feedback inhibition has been proposed to be crucial for the complex dynamics of olfactory network responses (18).

In addition to these inhibitory inputs arising from GC, it has been reported that MC lateral dendrites receive large excitatory inputs when either inhibition was antagonized or magnesium was removed from the external medium (19–22). In mammals, excitatory synapses onto MC have been localized exclusively to the apical dendritic tufts that receive primary sensory afferents (2, 4, 5, 23, 24). The origin of the excitatory inputs to the MC lateral dendrites therefore is debated. Isaacson (20) has proposed that this excitation depends on glutamate release from the MC themselves. However, it is unknown how the specificity for odor processing can be conserved if glutamate spillover alone governs excitatory transmission within the main olfactory bulb. Using a combination of *in vitro* whole-cell recordings and immunogold detection of glutamate, we explored the possibility that ionotropic glutamate receptors on MC could rather be activated by interneurons located in the GC layer. Such feedback excitation would provide an effective mechanism for temporal and spatial codings in olfactory information processing.

Materials and Methods

Slice Preparation. Experiments were performed on olfactory bulb slices obtained from 15- to 31-day-old anesthetized (halothane) Sprague–Dawley rats as described (16). Bulbs were rapidly removed and immediately placed in 4°C oxygenated artificial cerebrospinal fluid (ACSF) containing: 124 mM NaCl, 3 mM KCl, 2 mM $CaCl_2$, 1.3 mM $MgCl_2$, 25 mM $NaHCO_3$, 1.25 mM NaH_2PO_4, 10 mM D-glucose, pH 7.3 when bubbled with 95% O_2-5% CO_2 (310 mOsm). Horizontal slices (300 μm) were cut with a vibrating microslicer (Vibratome 1000; TPI, St Louis) and kept in oxygenated ACSF at 32°C for about 30 min and then at room temperature (20–22°C).

Electrophysiological Recordings. Patch electrodes with access resistance of 5–8 MΩ and 10–12 MΩ were used to record MC and GC, respectively, and they contained: 123 mM Cs-gluconate, 10 mM CsCl, 8 mM NaCl, 1 mM $CaCl_2$, 0.2 mM Cs-EGTA, 10 mM Na-Hepes, 10 mM D-glucose, 0.3 mM GTP, 2 mM Mg-ATP, 0.2 mM AMPc, pH 7.3 (290 mOsm). In some experiments, QX-314 (10 mM) was added to the internal solution to block Na currents in the MC. To evoke synaptic responses, stimuli (100-μs duration) were delivered through fine bipolar tungsten electrodes placed in the olfactory nerve layer or in the external plexiform layer (EPL).

L-glutamate (250 mM), prepared in distilled H_2O and adjusted to pH 8.2 with NaOH, was successively applied iontophoretically to the MC lateral dendrite or soma. No pharmacological differences were observed between these two locations (20- to 300-nA current application during 500 ms and 15 nA for continuous retention) through a 5–10 MΩ patch pipette by using a dual microiontophoresis current generator (World Precision Instruments, Astonbury, U.K.). Applications were performed every 20 s. All evoked currents were subtracted with the traces recorded in the Mg^{2+}-free external medium containing: 0.5 μM tetrodotoxin (TTX), 10 μM bicuculline methiodide (BMI), 100 μM picrotoxin (PTX), 10 μM 1,2,3,4-tetrahydro-6-nitro-2,3-dioxobenzo[*f*]quinoxaline-7-sulfonamide (NBQX), 100 μM D,L-2-amino-5-phosphonovaleric acid (APV), and 15 μM 5,7-dichlorokynurenic acid (dCK). L-glutamate also was applied

Abbreviations: APV, 2-amino-5-phosphonovaleric acid; BMI, bicuculline methiodide; CPP, 3-[(±)-2-carboxypiperazin-4-yl]propyl-1-phosphonate; dCK, 5,7-dichlorokynurenic acid; EPL, external plexiform layer; EPSC, excitatory postsynaptic current; 4-AP, 4-aminopyridine; GABA, γ-aminobutyric acid; GC, granule cells; I_A, A-type potassium current; IPSC, inhibitory postsynaptic current; MC, mitral cells; NBQX, 1,2,3,4-tetrahydro-6-nitro-2,3-dioxobenzo-[*f*]quinoxaline-7-sulfonamide; NMDA, *N*-methyl-D-aspartate; PTX, picrotoxin; TTX, tetrodotoxin.

†A.D. and A.C. contributed equally to this work.

¶To whom reprint requests should be addressed. E-mail: Pierre-Marie.Lledo@iaf.cnrs-gif.fr.

The publication costs of this article were defrayed in part by page charge payment. This article must therefore be hereby marked "*advertisement*" in accordance with 18 U.S.C. §1734 solely to indicate this fact.

NEUROBIOLOGY

iontophoretically (30- to 40-nA current application during 2.5 s and 10 nA for continuous retention) to the GC soma (stimulations were performed every 20 s). The electrode was placed in the GC layer at least 100 μm away from the MC layer to prevent any direct effect of glutamate on MC. Stimulation of GC by iontophoresis of glutamate was chosen because it prevents MC antidromic spike generation or centrifugal fibers stimulation. Glutamate application elicited by low current injection/long duration was the best way to prevent direct effect on MC and to promote spike generation by glutamate receptor activation. As control, we have performed GC current-clamp recordings to check that iontophoresis of glutamate was efficient in eliciting spikes even in the presence of APV and dCK (data not shown).

Synaptic responses were filtered at 1–5 kHz with an eight-pole Bessel filter, digitized at 4 kHz on a TL-1 interface (Axon Instruments, Foster City, CA), and collected on an IBM-compatible computer. On- and off-line data analyses were carried out with ACQUIS-1 (Gérard Sadoc, Centre National de la Recherche Scientifique). During all experiments, the access resistance (R_a) and the input membrane resistance (R_m) were monitored, and acquisition was terminated when these parameters changed more than 20%. Data are expressed as mean ± SEM, and for statistical comparisons we used a paired Student's t test.

When Lucifer yellow (0.4%) was added in the recording pipette no difference in the frequency of small excitatory postsynaptic currents (EPSCs) was observed between MC having their apical dendrite sectioned or not. However, the large spontaneous inward currents previously described were eliminated in apical dendrite-free MC (20–22, 25). Furthermore, kinetic analysis allows us to discriminate between EPSCs originating from the olfactory nerve and those from lateral dendrites. Drug solutions were bath-applied by using a gravity-driven perfusion system. NBQX, D,L-APV, 3-[(±)-2-carboxypiperazin-4-yl]propyl-1-phosphonate (CPP), MK-801, dCK, D-serine, AP7, and LY 235 959 were provided from Tocris; all other drugs and salts were purchased from Sigma.

Electron Microscopy Data. Postembedding immunocytochemistry was performed on ultrathin sections obtained from two adult Wistar rats after intracardiac perfusion with 2% dextran (molecular weight 70,000) followed by the fixative (2.5% glutaraldehyde + 1% paraformaldehyde in 0.1 M phosphate buffer, pH 7.4) under deep anesthesia (pentobarbital 50 mg/kg). Sections were incubated with previously characterized primary antibodies raised in rabbits against glutaraldehyde conjugates of glutamate or GABA (26, 27). Labeling was visualized by gold particles (mean diameter 15 nm), coupled to the secondary antibody. The relationship between gold particle density and the actual concentration of amino acid varied depending on the antibody or experimental conditions (26, 27). Specificity was assessed by using test sections containing glutaraldehyde conjugates of selected amino acids and revealed no cross reactivity of the antibodies except for a slight cross reactivity of the glutamate antiserum with glutamine (not shown). To quantify immunoreactivity associated with synaptic vesicles, locations of gold particles, centers of vesicles, and outlines of the profiles were digitized from electron micrographs by using a modified version of the program MICROTRACE as described (28, 29). Custom software was used to determine the intercenter distances from each gold particle to the nearest synaptic vesicle (30), sorting the distances into 20-nm bins (chosen arbitrarily as a distance slightly smaller that the theoretical resolution of the immunogold localization). The distribution was compared with that of distances from random points to synaptic vesicle centers (28, 29). The random points, 1,000 times the number of gold particles, were spread over the nerve terminal cytoplasm (areas occupied by mitochondria were excluded from the analysis). The statistical significance of the difference between the observed and expected (random points) distributions among three bins (0–20 nm, 20–40 nm, >40 nm) was evaluated by the χ^2 test for known distributions.

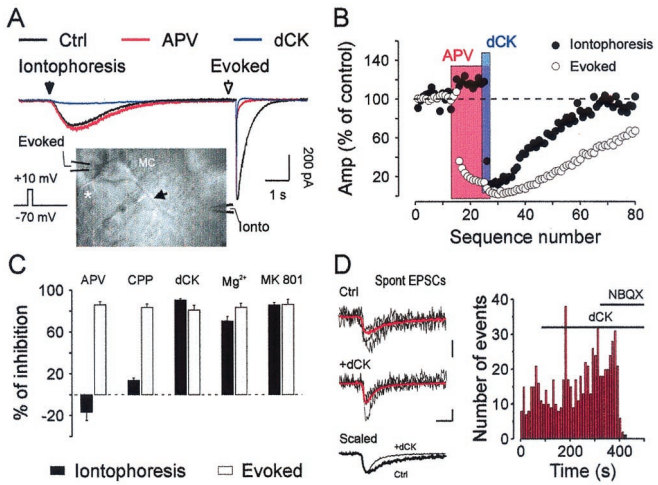

Fig. 1. MC lateral dendrites express NMDA receptors with unusual pharmacology. (*A*) Sequential iontophoresis of glutamate and voltage steps were performed on a MC. Brief glutamate application (filled arrowhead, 500 ms) elicited a direct inward current while a short depolarization applied through the recording electrode (open arrowhead; depolarizing currents were blanked) induced an evoked inward current. Recordings were performed in control conditions (Ctrl: black trace; 0 Mg^{2+}, 0.5 μM TTX, 10 μM BMI, 100 μM PTX, 10 μM NBQX). Red trace indicates application of D,L-APV (100 μM), and blue trace indicates application of 5,7-dCK (15 μM). Each trace is the average of five sweeps. (*Inset*) Infrared differential interference contrast image of a MC showing a lateral dendrite (arrow), the axon (*) and the location of the recording and ejecting pipettes. (*B*) Time course of the experiment illustrated in *A*. The colored boxes represent the duration of bath applications of the antagonists. (C) Summary graph showing the percentage of blockage induced by different NMDA receptor antagonists on iontophoretic (filled columns) and voltage-evoked (open columns) responses. Cells were recorded in the same external medium as in *A* supplemented with different NMDA receptor antagonists. The application of D,L-APV (100 μM) induced a clear blockade of the evoked response whereas iontophoretic responses were slightly potentiated (not statistically significant). Application of 1.3 mM Mg^{2+} inhibited both responses (a mean reduction of 70 ± 4%, $P < 0.0001$, $n = 10$ and 83 ± 4%, $P < 0.009$, $n = 6$, for iontophoresis and evoked responses, respectively). Application of 25 μM MK-801 also inhibited both responses (a mean reduction of 86 ± 2%, $P < 0.0001$, $n = 12$ and 86 ± 5%, $P < 0.04$, $n = 6$, for, respectively, iontophoresis and evoked responses). For iontophoresis, the control medium was supplemented with D,L-APV (100 μM). (*D*) A MC exhibits spontaneous EPSCs (spont EPSCs) mediated in part by APV-resistant NMDA receptors. MC recorded under control conditions: 0 Mg^{2+}, 10 μM BMI, 100 μM PTX, 10 μM NBQX, and 100 μM D,L-APV showed spontaneous EPSCs (*Top*, the red trace represents the average of 50 events whereas the other traces represent single events). Bath application of 5,7-dCK (15 μM) did not affect their frequency (see histogram; bin 10 s) but decreased their decay time constant (*Middle*; the red trace represents the average of 70 events). (*Bottom*) The two averaged traces are scaled to match peak amplitudes. The remaining component of the EPSC is mediated by the non-NMDA receptors because they were totally blocked by NBQX (10 μM). (Scale bars: 2 ms and 10 pA; see Table 1, which is published as supplemental data on the PNAS web site, www.pnas.org.)

Results

Glutamate released from individual MC dendrites is proposed to have both local and diffuse actions resulting respectively in self- and lateral excitation of MC via the activation of *N*-methyl-D-aspartate (NMDA) receptors (20–22). To locate and study more precisely these receptors, we began by iontophoretically applying L-glutamate at the somato-dendritic compartment of MC (Fig. 1). Rat olfactory bulb slices were bathed in Mg^{2+}-free buffer to

remove the antagonistic action of Mg^{2+} on NMDA channels, supplemented with TTX (0.5 μM) to block Na^+ action potentials. Whole-cell patch-clamp recordings in the presence of the non-NMDA receptor antagonist NBQX (10 μM) and BMI (10–20 μM) with PTX (100 μM) and strychnine (30 μM), to block both GABA type A and glycine receptors, revealed an inward current in response to glutamate iontophoresis (Fig. 1*A*). Focal application of glutamate to MC always elicited responses but small ($\approx$20 μm) displacements of the ejecting pipette from the soma and along the lateral dendrite either increased or decreased the amplitude of the responses (data not shown; n = 6). This observation indicates an uneven distribution of functional glutamate receptors activated by the iontophoresis. To compare iontophoretic responses with synaptically released glutamate, MC were subjected to a brief depolarization (from -70 to $+10$ mV, 25 ms), which evoked endogenous glutamate release (refs. 7, 8, and 22; Fig. 1 *A* and *B*). Under these conditions, the short depolarizing step evoked after the iontophoresis application induced an inward current interpreted as self-excitation produced by locally released glutamate (19–22).

APV Reveals an Unusual NMDA Receptor in MC. We used specific antagonists of ionotropic glutamate receptors to further characterize iontophoretic responses and self-excitation induced by exogenous and endogenous glutamate, respectively. The NMDA receptor antagonist D,L-APV was first added to the external recording medium already containing NBQX, PTX, and BMI (Fig. 1 *A–C*). Surprisingly, whereas the application of APV (100 μM) was able to nearly abolish the voltage pulse-evoked responses as reported by others (86 $\pm$ 3% reduction, n = 9; $P <$ 0.02), iontophoretic glutamate responses were either unaffected or even potentiated in the presence of APV (17 $\pm$ 8% increase, n = 18; P = 0.16; see Fig. 1 *A* and *B*). These results were partially mimicked by the use of a different competitive NMDA receptor antagonist for the glutamate binding site CPP. In all cells tested, bath-applied CPP (10 μM) strongly and reversibly reduced the voltage pulse-evoked current (84 $\pm$ 3% reduction; n = 5; $P < 5 \times 10^{-5}$) whereas the iontophoresis-induced currents were only slightly affected (14 $\pm$ 2% reduction, n = 5; $P <$ 0.02; Fig. 1*C*). Therefore, our protocol revealed the presence of glutamate receptors located on the somato-dendritic compartment of MC (whose activation resulted in an APV-resistant current) that were clearly distinct from those activated by voltage pulses (resulting in an APV-sensitive current). The APV-resistant inward current seen with our iontophoresis protocol was, however, mediated by activation of NMDA receptors because bath application of a competitive NMDA receptor antagonist specific for the glycine binding site, dCK (15 μM), dramatically reduced its amplitude by 90.4 $\pm$ 1.4% (n = 14, $P < 2 \times 10^{-7}$; Fig. 1 *A–C*).

To further characterize the properties of the APV-resistant inward current, we studied its voltage dependency (supplemental Fig. 6). In the presence of external Mg^{2+} and APV, the current induced by bath application of NMDA (100 μM) showed the typical rectification characteristic of NMDA currents and was found to be blocked by dCK application (data not shown; n = 4). Furthermore, we used a panel of other blockers known to specifically target different sites of the NMDA receptors. The results from experiments designed to compare iontophoresis-induced and voltage-evoked responses are summarized in Fig. 1*C*. The two NMDA channel pore blockers, MK-801 (25 μM) and Mg^{2+} (1.3 mM), strongly reduced both responses. Similar iontophoretic applications of glutamate were made onto the soma of GC (bathed with 0 Mg^{2+}, TTX, BMI, PTX, strychnine, and NBQX) to test the effectiveness of APV. In contrast to MC, iontophoretic applications on GC elicited an NMDA current, which was fully blocked by 50 μM D-APV (supplemental Fig. 6; n = 4). This finding rules out the possibility that APV, a competitive antagonist, was inefficient due to a massive application of exogenous glutamate (supplemental Fig. 7).

We further tested the relative sensitivity of NMDA receptors to bath application of APV in two different synapses. First, olfactory nerve stimulations were applied to recruit glutamatergic synapses made between olfactory nerve axons and apical dendrites of MC or tufted cells. Second, stimulations in the EPL were used to evoke excitatory dendrodendritic synaptic responses between the MC or tufted cell lateral dendrites and the dendrites of GC. As reported by others (7, 8, 13, 25, 31–35), an APV-sensitive component was detected at both synapses. Furthermore, in contrast to results obtained during iontophoresis, when APV and NBQX were sequentially applied, a total blockade was seen for the two synaptic responses, indicating absence of APV-resistant NMDA current at these synapses (data not shown; n = 7 and 4, respectively).

From these results, we conclude that iontophoretically applied glutamate reveals the presence of an unusual type of NMDA receptor located on the somato-dendritic compartment of MC. We then investigated whether this APV-resistant NMDA component could participate in synaptic transmission. For this purpose, MC were voltage-clamped at -70 mV, in part to reduce the probability of spontaneous release of glutamate, and recorded in Mg^{2+}-free saline supplemented with BMI (10–20 μM), PTX (100 μM), and D,L-APV (100 μM). Under these conditions, spontaneous EPSCs reflecting the activation of both non-NMDA and NMDA glutamate receptors were detected (Fig. 1*D*; n = 7) even when the apical MC dendrite was truncated. Application of dCK (15 μM) caused a marked change in the kinetics of these spontaneous events, revealing that the non-NMDA receptor-mediated component had faster decay kinetics (3.8 $\pm$ 0.6 ms in APV vs. 1.4 $\pm$ 0.2 ms in APV + dCK; $P <$ 0.02; see also traces in Fig. 1*D*). Subsequent addition of NBQX (10 μM) eliminated the remaining synaptic activity (n = 5).

MC Are Excited by Interneurons from the GC Layer. It is noteworthy that these results contrast with previous findings on self-excitation, which report only an NMDA component (19–22). However, they are supported by recordings of voltage pulse-induced responses found to be sensitive to 10 μM NBQX (a mean reduction of 13 $\pm$ 5%, $P <$ 0.009, n = 10; not shown; see also ref. 51). Because MC dendrites of mammals do not make any synaptic contacts with other MC (2), it has been proposed that extrasynaptic spillover of glutamate released from these cells can evoke self-excitation and excitatory transmission between neighboring MC (19–22). However, only an APV-sensitive component was believed to mediate these effects. Thus, the source of glutamate able to activate both non-NMDA and NMDA receptors in the presence of APV must be different from the one previously thought. To identify its origin, we performed immunocytochemical studies to detect glutamate-containing spines within the olfactory bulb network.

Ultrastructural immunogold cytochemistry revealed glutamate-like immunoreactivity (Glu-LI) in dendritic terminals making reciprocal synapses with MC dendrites in the EPL. Based on their morphological features (2, 3), these terminals were identified as GC spines (Fig. 2*A*). As previously reported for GC spines (36), the cross-sectioned area occupied by mitochondria represented 4.1 $\pm$ 1.1% of the total area of the profiles (n = 24). In another set of experiments, immunogold detection of GABA was performed, and anatomically similar spines were found to be GABA-like immunoreactive (GABA-LI) (Fig. 2*B*), in accordance with their inhibitory function (7–10, 37, 38). In presynaptic profiles, glutamate may serve as GABA precursor. Alternatively, it could be used as a transmitter that would imply a vesicular localization of Glu-LI (30, 39, 40). This issue was addressed by calculating intercenter distances between gold particles and the nearest synaptic vesicle (28, 29). In GC spines labeled for glutamate, short distances (less than 20 nm) are significantly

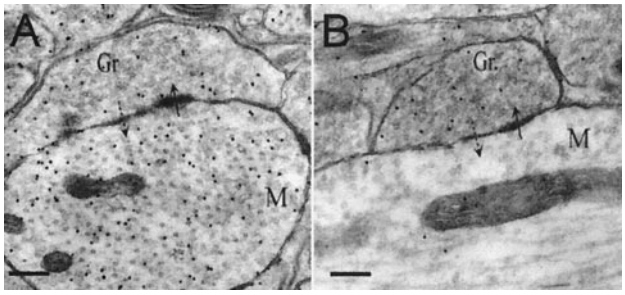

Fig. 2. Electron micrographs showing immunogold labeling for glutamate (Glu-LI, *A*) or GABA (GABA-LI, *B*) in reciprocal synapses between GC spines (Gr) and MC dendrites (M) in the EPL. The mitral to granule contact is asymmetric (solid arrow) and the granule to mitral contact is symmetric (dotted arrow). Glu-LI is found in MC and GC (*A*). GABA-LI is localized to the GC (*B*). Particle densities (particles/μm^2) for Glu-LI are 63.1 ± 5.8 over M and 86.5 ± 5.2 over Gr (mean ± SE). Particle densities for GABA-LI are 9.7 ± 3.3 over M and 30.1 ± 2.8 over Gr. Background noise, assessed over empty resin, was of 4 ± 2.3 particles/μm^2 for Glu-LI and 3.1 ± 0.2 particles/μm^2 for GABA-LI. (Scale bars: 240 nm.) Electron micrographs were obtained from a Phillips CM120 electron microscope at the Université Claude Bernard-Lyon.

more frequent than expected from a random distribution of gold particles over the spines, indicating that glutamate is associated with vesicles (Fig. 3*A*). In GABA-LI-positive GC spines, gold particles were similarly found to be significantly associated with the synaptic vesicles (Fig. 3*B*). A positive control for vesicular glutamate labeling was obtained from the glutamatergic primary olfactory terminals (41), showing a nonrandom intercenter distance distribution shifted toward short distances (Fig. 3*C*). By contrast, axon terminals from centrifugal neurons, thought to be principally nonglutamatergic and to impinge on GC dendrites within the EPL (3, 42), exhibit a randomly distributed Glu-LI (Fig. 3*D*). Our data suggest that glutamate is preferentially located in vesicles contained in presynaptic GC spines.

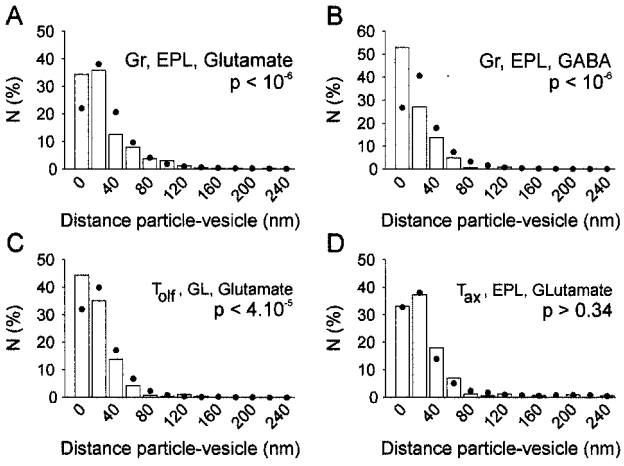

Fig. 3. Quantification of the association of immunoreactivity with synaptic vesicles. Measurements of intercenter distances between each gold particle and the nearest synaptic vesicle were done, and distances were sorted into bins of 20 nm (columns), the *y* axis showing percent of total in each bin. Distances to the vesicle center from points randomly distributed over the terminal (●) also were calculated (see refs. 40 and 41). (*A*) Short distances were significantly more represented in experimental distributions compared with random distributions in GC spines labeled for glutamate, indicating that Glu-LI was associated with synaptic vesicles. (*B*) GABA-LI also was localized to vesicles in GC (Gr) spines. (*C*) The same was true for Glu-LI in the primary olfactory axon terminals (Tolf) within the glomeruli (GL). (*D*) By contrast, axon terminals (Tax) from centrifugal neurons making asymmetric contacts with GC dendrites in the EPL (3) contained glutamate not associated with synaptic vesicles (χ^2 test). Gr Glutamate: 500 gold particles (24 spines); Gr GABA: 260 gold particles (21 spines); Tolf glutamate: 387 gold particles (13 terminals); Tax: 282 gold particles (11 terminals). Bins not shown amounted to less than 2% of total. χ^2 values for comparison of gold particles distribution with random points distribution: Gr (EPL) glutamate, 49.6; Gr (EPL) GABA, 87.6; Tolf GL glutamate, 20.7; Tax EPL glutamate, 2.1.

Activation of GC Elicits Excitatory Synaptic Events in MC. We then asked whether this vesicular glutamate could be released by direct activation of GC. To address this question, MC were recorded and GC were directly stimulated by using somatic glutamate application. Fig. 4*A* illustrates a MC recording during local stimulations of GC. In Mg^{2+}-free saline, granule cell stimulation elicited large synaptic responses in MC (Fig. 4*B1*). Because the recording pipette contained a Cs/gluconate-based internal solution that sets the reversal potential for GABA type A receptor-mediated currents near −50 mV, inhibitory postsynaptic currents (IPSCs) were seen as inward events at a holding potential of −70 mV. These evoked synaptic currents were reduced by adding PTX (100 μM) with BMI (10–20 μM), indicating they were mediated by MC GABA type A receptors (Fig. 4*B1*). Focal stimulations of GC trigger evoked synaptic responses in MC resulting from the summation of many individual IPSCs (Fig. 4*B2*). In the cell displayed in Fig. 4*B3*, the average IPSC (n = 90 events) had a peak amplitude of −38 pA with a decay time constant of 9 ms. Thus, inhibitory inputs onto MC can be reliably activated by glutamate applied to GC soma (see Fig. 4*B1*). Interestingly, after the blockade of GABA type A receptors, large spontaneously occurring excitatory currents appeared on MC. As reported (20–22, 25), bath application of D,L-APV (100 μM) abolished these events (Fig. 4*A*) but revealed slow inward currents and discrete synaptic events that could still be detected in the presence of APV and IPSCs antagonists (Fig. 4 *C1* and *C2*). As shown by the application of dCK, these synaptic currents were excitatory (a mean amplitude of −10 pA) and were mediated by activation of both non-NMDA and NMDA receptors (Fig. 4*C3*). After addition of dCK, the averaged EPSC had a fast decay time constant (3.6 ms) characteristic of non-NMDA receptor-mediated EPSC (see Fig. 1*D*). Moreover, the slow inward current was reversibly reduced either by 25 μM MK-801 or 15 μM dCK (n = 5; Fig. 4*D*). The possibility that this slow inward response was due to glutamate spreading directly onto MC was discarded on the following grounds. Given the separation between iontophoresis and recording electrodes (at least 100 μm), its seems unlikely that glutamate applied in the GC layer could diffuse so far away. Second, bath application of TTX (0.5 μM) completely blocked this evoked response (n = 4), demonstrating that stimulation with iontophoresis of glutamate requires neuronal spiking (Fig. 4*D*).

We next took advantage of the unique way in which the transient A-type potassium current (I_A) specifically regulates neurotransmitter release from GC, to unambiguously locate the source of glutamate activating ionotropic receptors on MC. Recently, the transient I_A has been demonstrated to prevent GABA release mediated by non-NMDA receptors (13). We investigated whether I_A also could be responsible for limiting feedback excitation. Depolarizing the recorded MC (25 ms from −70 to + 10 mV) in 1.3 mM Mg^{2+} saline containing BMI- and PTX-induced reciprocal EPSCs. As expected if glutamate originates from GC, addition of a specific antagonist of I_A, 4-aminopyridine (4-AP; 2.5–5 mM) markedly increased the amplitude of the reciprocal excitation (76 ± 13% increase, n = 5; $P < 0.015$; Fig. 5*A*). Similarly, we have tested whether glutamate released by GC also could be involved in lateral excitation between MC through synaptically shared GC. Electrical stimulations were delivered at the border between the glomerular layer and EPL (see Fig. 5*B* for the experimental configuration) to activate neighboring apical MC dendrites. To avoid direct stimulation of the recorded MC (and therefore reciprocal excitation), the sodium channel antagonist QX-314 (10 mM) was added to the

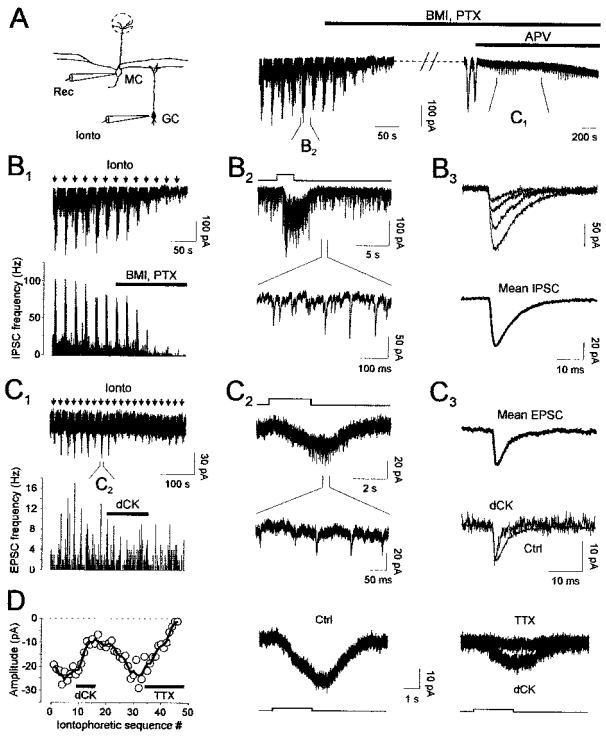

Fig. 4. Stimulation of GC elicited glutamate release onto MC. (*A*) MC are recorded while GC are stimulated by the iontophoresis of glutamate. Traces represent the time course of the experiment and were cut during application of BMI (10 μM) and PTX (100 μM) because they produced large inward currents that were blocked by D,L-APV (100 μM). (*B 1–3*) GC stimulation increases GABA release onto MC. (*B1*) Experiment performed in 0-Mg^{2+} during iontophoresis stimulations (black arrows). The histogram represents the IPSC frequency during the recording (bin 1 s). BMI/PTX reduced those events. (*B2*) The stimulation increases the IPSC frequency (*Upper*, see also the histogram in *B1*; the step represents iontophoretical applications). (*Lower*) Shown is an expanded time scale part of the upper trace showing individual synaptic events. (*B3*) Unitary IPSC (*Upper*) and the average of 90 events (*Lower*) are presented. (*C 1–3*) GC stimulation increases glutamate release onto MC. (*C1*) The same cell as in *B* was recorded in: 0 Mg^{2+}, 10 μM BMI, 100 μM PTX, and 100 μM D,L-APV (black arrows indicate iontophoretic stimulations). The histogram represents EPSC frequency during the recording (bin 1 s). The bar shows the duration of dCK (15 μM) application. (*C2*) Traces showing the effect of one iontophoretic stimulation. Stimulation of GC induced a slow inward current (*Upper*) on the top of which discrete EPSCs could be seen (lower trace represents an expanded part of the upper one; see also histogram in *C1*; the step represents the iontophoretic application). (*C3*) Averages of EPSC recorded with or without dCK (15 μM). (*Upper*) Average of 35 events recorded before dCK application. (*Lower*) Changes in the decay time after dCK application (the average in dCK represents the average of 20 events). (*D*) (*Left*) Graph represents the amplitude of the iontophoretic evoked inward current recorded during the time course of the experiment depicted in *C1*. Bath application of dCK (15 μM) revealed that this current was mediated in part by APV-resistant NMDA receptors. After washout of this drug, bath application of TTX (0.5 μM) completely abolished the current, confirming that it was due to the excitation of GC rather than a direct effect on the MC dendrites. The traces showing the drug effects are the average of five sweeps.

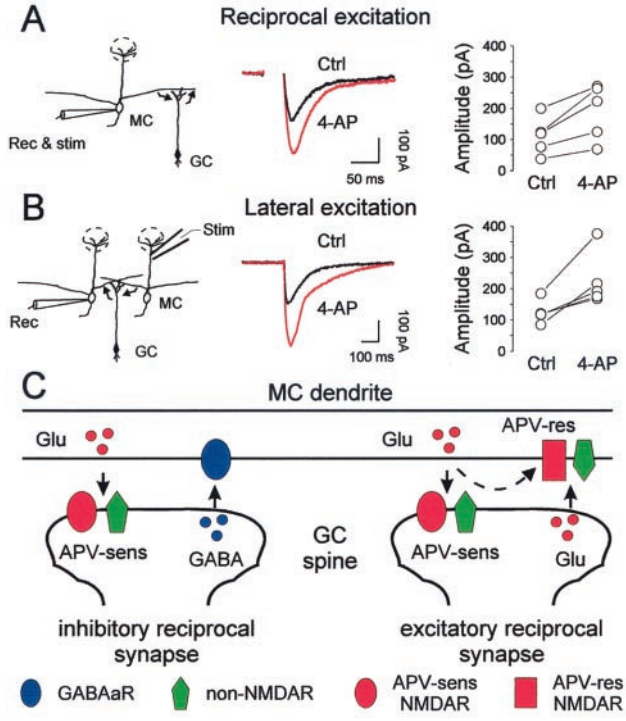

Fig. 5. Glutamate released by GC mediates both reciprocal and lateral excitation. (*A*) The reciprocal excitation elicited by depolarization of the recorded MC (*Left*) is recorded in control conditions (1.3 mM Mg^{2+} with 10 μM BMI and 100 μM PTX). 4-AP (5 mM) increased significantly the amplitude response (middle traces) in five tested cells. (*Right*) Summary graph of the 4-AP effect. (*B*) EPL stimulation triggered lateral excitation recorded in control conditions containing Mg^{2+} (1.3 mM) with BMI (10 μM), PTX (100 μM), and QX-314 (10 mM) in the recording pipette. 4-AP (5 mM) also increased significantly the amplitude response (middle traces) in five tested cells. (*Right*) Summary graph of the 4-AP effect. (*C*) Model representing the two reciprocal synapses mediated by the same or different subtypes of GC. The term reciprocal implies that MC releases glutamate, activating both non-NMDA and APV-sensitive NMDA receptors, which trigger neurotransmitter release by GC spines at the same synapse (arrows). Glutamate from GC activates both non-NMDA and APV-resistant NMDA receptors on the MC dendrites. It is possible that glutamate released by MC could activate directly the MC glutamate receptors (dotted arrow) although our data indicate a moderate contribution (supplemental Fig. 8).

patch pipette solution, and MC were always recorded at a certain distance from the stimulating electrodes (at least 200 μm). Under these conditions, the amplitude of lateral excitation was similarly potentiated by the blockade of I_A (86 $\pm$ 35% increase, $n = 5$; $P < 0.02$; Fig. 5*B*).

Discussion

Synaptic transmission at dendrodendritic synapses between MC and GC provides a fast inhibitory feedback onto MC. Our results showed that GC also contribute to recurrent excitation of relay neurons. These interneurons release glutamate, which activates both AMPA and APV-insensitive NMDA receptors located on the soma and lateral dendrites of MC. This recurrent excitation onto relay neurons is likely to play an important role in prolonging periods of phasic firing in MC.

MC Lateral Dendrites Receive Excitatory Inputs from GC. The idea that odor information is encoded by activity distributed across the olfactory bulb neuronal network is consistent with physiological experiments (43–45), but the underlying mechanism remains poorly documented. Through their tangential extent and numerous dendrodendritic reciprocal synapses with granule cell dendrites (2, 4, 5), MC lateral dendrites provide a key anatomical element for distributing information throughout the entire olfactory bulb. The temporal and spatial shaping of olfactory bulb output is strongly influenced by the amplitude and duration of the dendrodendritic inhibition (44, 45). However, theoretical studies have suggested that excitation also may play an important role in temporal shaping of neuronal discharges (46). Experimentally, excitatory events in MC can be induced by antidromic stimulations (19, 25) or intracellular depolarizing currents (20–22, 51), demon-

strating the presence of recurrent excitatory inputs to MC mediated by NMDA receptors. Preembedding immunocytochemistry has demonstrated ionotropic glutamate receptors in MC dendrites (47–49), but a recent postembedding immunogold analysis revealed no labeling for NMDA receptors and only occasional labeling for AMPA receptors on MC dendrite membranes facing GC spines (50). The lack of immunodetection of NMDA receptors could be related to the pharmacological profile reported here. Alternatively, these receptors may be scattered rather than clustered, preventing easy detection by immunogold labeling. A similar mechanism may explain why non-NMDA receptors that contribute to MC excitation have escaped immunogold detection.

The major synaptic contacts of secondary MC dendrites within the EPL are reciprocal synapses with GC spines (1, 37, 38). However, a small subpopulation of interneurons distinct from GC and expressing parvalbumin also makes reciprocal contacts with MC dendrites in the EPL (36). These terminals were found to be rich in mitochondria and thus can be distinguished from GC spines. Furthermore, parvalbumin-positive cell bodies and processes are confined to the EPL whereas glutamate-mediated events in MC were recorded after stimulations applied in the GC layer. On these grounds, the large majority of the cellular profiles, detected by Glu-LI and participating in reciprocal synapses with MC, clearly belongs to the GC population. We show here that dendritically released glutamate from MC activates local interneurons in the GC layer, through NMDA (APV-sensitive) receptors. Then, GC subsequently excite MC by releasing glutamate on both non-NMDA receptors and an APV-resistant subtype of NMDA receptor (see model in Fig. 5*C*). Because feedback excitation is almost completely blocked by APV, it would appear that the APV-resistant receptors are not reached by glutamate of MC origin.

An Excitatory Synaptic Connection in the Main Olfactory Bulb. Recent studies have proposed that recurrent excitation of MC is mediated by glutamate that escapes from synapses to activate exclusively extrasynaptic NMDA receptors. However, it is questionable whether this spillover-mediated transmission plays a functionally important role in synaptic communication because previous studies were performed in the absence of external Mg^{2+}. Furthermore, the presence of non-NMDA synaptic events in MC lateral dendrites reported here is in apparent contrast with the spillover hypothesis because activation of non-NMDA receptors requires high concentration of glutamate, probably achieved only within the synaptic cleft. Thus, non-NMDA synaptic events indicate that transmission at the excitatory dendrodendritic synapses is rather "point to point," with glutamate being released from both MC and GC. Because GC vastly outnumber MC, the activation of a single MC could result in robust reciprocal dendrodendritic excitation. Whether the same or different GC release both glutamate and GABA is currently unknown and should be specifically addressed in the near future.

In conclusion, we have demonstrated that the main population of bulbar local interneurons, previously thought to be exclusively inhibitory, provides both strong feedback and lateral excitation on MC through a dendrodendritic excitatory reciprocal synapse. This finding points to an unexpected degree of complexity of the neuronal network of the main olfactory bulb and forces us to revise current concepts about the way the GC regulate the olfactory bulb output.

We thank B. Riber and K. M. Gujord for excellent technical assistance and F. Jourdan and H. McLean for comments on the manuscript. This work was supported in part by Centre National de Recherche Scientifique (A.D. and P.-M.L.), a grant from the French Ministère de la Recherche et de l'Enseignement (A.C.) and the Ministère de l'Education Nationale, de la Recherche et de la Technologie (ACI Biologie du Développement et Physiologie Intégrative 2000) (to P.-M.L.), a fellowship under the Organization for Economic Cooperation and Development Cooperative Research Program and Biological Resource Management for Sustainable Agricultural Systems (A.D.), and the Norwegian Research Council (J.G.B., O.P.O., and J.S.-M.).

1. Rall, W., Shepherd, G. W., Reese, T. S. & Brightman, M. W. (1966) *Exp. Neurol.* **14,** 44–56.
2. Price, J. L. & Powell, T. P. S. (1970) *J. Cell Sci.* **7,** 631–651.
3. Price, J. L. & Powell, T. P. S. (1970) *J. Cell Sci.* **7,** 91–123.
4. Pinching, A. J. & Powell, T. P. S. (1971) *J. Cell Sci.* **9,** 347–377.
5. Shepherd, G. M. (1972) *Physiol. Rev.* **52,** 864–917.
6. Trombley, P. & Shepherd, G. M. (1993) *Curr. Opin. Neurobiol.* **3,** 540–547.
7. Schoppa, N. E., Kinzie, J. M., Sahara, Y., Segerson, T. P. & Westbrook, G. L. (1998) *J. Neurosci.* **18,** 6790–6802.
8. Isaacson, J. S. & Strowbridge, B. W. (1998) *Neuron* **20,** 749–761.
9. Nowycky, M. C., Mori, K. & Shepherd, G. M. (1981) *J. Neurophysiol.* **46,** 639–648.
10. Jahr, C. E. & Nicoll, R. A. (1982) *J. Physiol. (London)* **326,** 213–234.
11. Scott, J. W., Wellis, D. P., Riggott, M. J. & Buonviso, N. (1993) *Microsc. Res. Tech.* **24,** 142–156.
12. Yokoi, M., Mori, K. & Nakanishi, S. (1995) *Proc. Natl. Acad. Sci. USA* **92,** 3371–3375.
13. Schoppa, N. E. & Westbrook, G. L. (1999) *Nat. Neurosci.* **2,** 1106–1113.
14. Shepherd, G. M. & Greer, C. A. (1998) in *The Synaptic Organization of the Brain*, ed. Shepherd, G. M. (Oxford Univ. Press, New York), 4th Ed., pp. 159–203.
15. Buonviso, N., Chaput, M. A. & Berthommier, F. (1992) *J. Neurophysiol.* **68,** 417–424.
16. Desmaisons, D., Vincent, J.-D. & Ledo, P.-M. *(1999) J. Neurosci.* **19**, 10727–10737.
17. Kashiwadani, K., Sasaki, Y. F., Uchida, N. & Mori, K. (1999) *J. Neurophysiol.* **82,** 1786–1792.
18. Wehr, M. & Laurent, G. (1996) *Nature (London)* **384,** 162–166.
19. Nicoll, R. A. & Jahr, C. E. (1982) *Nature (London)* **296,** 441–444.
20. Isaacson, J. S. (1999) *Neuron* **23,** 377–384.
21. Aroniadou-Anderjaska, V., Ennis, M. & Shipley, M. T. (1999) *J. Neurophysiol.* **82,** 489–494.
22. Friedman, D. & Strowbridge, B. W. (2000) *J. Neurophysiol.* **84,** 39–50.
23. White, E. L. (1972) *Brain Res.* **37,** 69–80.
24. Kosaka, K., Toida, K., Margolis, F. L. & Kosaka, T. (1997) *Neuroscience* **76,** 775–786.
25. Carlson, G. C., Shipley, M. T. & Keller, A. (2000) *J. Neurosci.* **20,** 2011–2021.
26. Ottersen, O. P. (1989) *Anat. Embryol.* **180,** 1–15.
27. Storm-Mathisen, J. & Ottersen, O. P. (1990) *J. Histochem. Cytochem.* **38,** 1733–1743.
28. Leergaard, T. B. & Bjaalie, J. G. (1995) *Neurosci. Res.* **22,** 231–243.
29. Chaudhry, F. A., Reimer, R. J., Bellocchio, E. E., Danbolt, N. C., Olsen, K. K., Edwards, R. H. & Storm-Mathisen, J. (1998) *J. Neurosci.* **18,** 9733–9750.
30. Gundersen, V., Chaudhry, F. A., Bjaalie, J. G., Fonnum, F., Ottersen, O. P. & Storm-Mathisen, J. (1998) *J. Neurosci.* **18,** 6059–6070.
31. Ennis, M., Zimmer, L. A. & Shipley, M. T. (1996) *NeuroReport* **7,** 989–992.
32. Aroniadou-Anderjaska, V., Ennis, M. & Shipley, M. T. (1997) *Neuroscience* **79,** 425–434.
33. Chen, W. R. & Shepherd, G. M. (1997) *Brain Res.* **745,** 189–196.
34. Keller, A., Yagodin, A., Aroniadou-Anderjaska, V., Zimmer, L. A., Ennis, M., Sheppard, N. F. & Shipley, M. T. (1998) *J. Neurosci.* **18,** 2602–2612.
35. Halabisky, B., Friedman, D., Radojicic, M. & Strowbridge, B. W. (2000) *J. Neurosci.* **20,** 5124–5134.
36. Toida, K., Kosaka, K., Heizmann, C. W. & Kosaka, T. (1996) *Neuroscience* **72,** 449–466.
37. Mori, K. & Tagaki, S. F. (1978) *J. Physiol. (London)* **279,** 569–588.
38. Jahr, C. E. & Nicoll, R. A. (1980) *Science* **207,** 1473–1475.
39. Storm-Mathisen, J., Leknes, A. K., Bore, A. T., Vaaland, J. F., Edminson, P., Haug, F. & Ottersen, O. P. (1983) *Nature (London)* **301,** 517–520.
40. Ottersen, O. P. & Storm-Mathisen, J. (1984) *Handbook of Chemical Neuroantomy* (Elsevier, Amsterdam), pp. 141–246.
41. Didier, A., Ottersen, O. P. & Storm-Mathisen. J. (1994) *NeuroReport* **6,** 145–148.
42. Halasz, H. & Shepherd, G. M. (1983) *Neuroscience* **10,** 579–619.
43. Cinelli, A. R., Hamilton, K. A. & Kauer, J. S. (1995) *J. Neurophysiol.* **73,** 2053–2207.
44. Laurent, G. (1999) *Science* **286,** 723–728.
45. Mori, K., Nagao, H. & Yoshihara, Y. (1999) *Science* **286,** 711–715.
46. Gonzalez-Estrada, M. T. & Freeman, W. T. (1980) *Brain Res.* **202,** 373–386.
47. Petralia, R. S., Yokotani, N. & Wenthold, R. J. (1994) *J. Neurosci.* **14,** 667–696.
48. Petralia, R. S., Wang, Y. X. & Wenthold, R. J. (1994) *J. Neurosci.* **14,** 6102–6120.
49. Montague, A. A. & Greer, C. A. (1999) *J. Comp. Neurol.* **405,** 233–246.
50. Sassoè-Pognetto, M. & Ottersen, O. P. (2000) *J. Neurosci.* **20,** 2192–2201.
51. Salin, P. A., Lledo, P. M., Vincent, J. D. & Charjak, S. (2001) *J. Neurophysiol.* **85,** 1275–1282.